Chiral hedgehog textures in two-dimensional *XY*-like ordered domains

Kok-Kiong Loh
Department of Physics, University of California at Los Angeles, Los Angeles, California 90095-1547

Isabelle Kraus
Institut de Physique et Chimie des Matériaux, Groupe des Matériaux Organiques, Unité Mixte CNRS–Université Louis Pasteur, 23 rue du Loess, F-67037 Strasbourg Cedex, France

Robert B. Meyer
The Martin Fisher School of Physics, Brandeis University, Waltham, Massachusetts 02254-9110
(Received 27 August 1999; revised manuscript received 25 June 2000)

The textures associated with a point defect centered in a circular domain of a thin film with *XY*-like ordering have been analyzed. The family of equilibrium textures, both stable and metastable, can be classified by a new radial topological number in addition to the winding number of the defect. Chiral textures are supported in an achiral system as a result of spontaneously broken chiral symmetry. Among these chiral textures, our theoretical analysis accurately describes two categories of recently discovered ''reversing spiral'' textures, ones that are energetically stable and metastable.

PACS number(s): 61.30.−v, 68.10.Cr, 68.18.+p, 68.55.Ln

Thin films of elongated molecules with tilt ordering, including smectic-*C* liquid crystals and dense fluid phases of amphiphiles deposited on water, very often possess fascinating distributions of the tilt azimuth. The organization of the tilt azimuth is referred to as the texture and can be observed by polarized light microscopy or Brewster angle microscopy. Many classes of these textures have been found experimentally, like stripes [1], stars [2], boojums [3], and hedgehogs [4]. These examples are observed in Langmuir monolayers composed of molecules that are symmetric under in-plane reflection, or achiral. Recently, more attention has been paid to the hedgehog patterns, obtained in a circular domain with a central point defect. The reversing spiral is one of the spectacular hedgehog textures discovered in a chiral tilted smectic-*C* liquid-crystal film on water [5]. Let us emphasize that both systems described above are polar, they are not symmetric under 180° rotation about an in-plane axis. The tilt azimuth can be represented by a two-dimensional vector $\hat{c}$, the projection onto the film of the elongated molecules, analogous to the order parameter of an *XY* model. Textures in two-dimensional *XY*-like systems have attracted a good deal of attention. A brief theoretical account based on a perturbative approach of hedgehogs in achiral monolayers can be found in Ref. [6]. The stability of the hedgehog configuration in an isotropic and achiral system has also been investigated [7]. Spiral textures in an achiral system have been studied in the small distortion regime [8]. Although a theoretical approach to solutions for hedgehog textures is given in Ref. [5], to the best of our knowledge, a systematic discussion of hedgehog textures in a chiral system has not been presented.

In this paper, we study a generic model [9] for the texture in a circular domain of a two-dimensional *XY*-like system. We have found a family of equilibrium configurations that can be classified by a new topological number analogous to the winding number that classifies a two-dimensional point defect [10]. When a system is achiral, these metastable configurations can be chiral as a result of spontaneously broken chiral symmetry. When chirality is explicitly introduced, more complex equilibrium textures result. The crossed polarizer images generated from the theoretical textures are in excellent agreement with the pictures taken experimentally. The starting point of our investigation is the following elastic energy of a chiral polar film with tilt ordering:

$$H[\hat{c}] = \tfrac{1}{2}\int_{\Omega} dA[K_s|\nabla\cdot\hat{c}|^2 + K_{sb}(\nabla\cdot\hat{c})(\nabla\times\hat{c}\cdot\hat{z}) + K_b|\nabla\times\hat{c}\cdot\hat{z}|^2] + \oint_{\Gamma} ds\,\sigma(\vartheta-\Theta). \quad (1)$$

It is computed for a circular area Ω containing the ordered medium enclosed by the boundary Γ. The unit vector $\hat{z}$ points normal to the film. The quantities K_b and K_s are, respectively, the bend and splay elastic moduli, $\hat{c}\equiv\hat{x}\cos\Theta + \hat{y}\sin\Theta$ is the order parameter of the system, Θ is the angle between $\hat{c}$ and the x axis, and ϑ is the angle between the outward normal to Γ and the x axis. The anisotropic line tension $\sigma(\phi)$ can formally be expanded as $\sigma_0 + \Sigma_n(a_n\cos n\phi + c_n\sin n\phi)$. We will consider only the first few coefficients in the expansion. The first-order terms are a_1 for polar films and c_1 for chiral systems. When the system is nonpolar, a_1 vanishes and a_2 must be considered. The coefficient c_2 is relevant when the system is both polar and chiral, but it will be neglected because a_1 and c_1 are nonzero for such a system. The cross term $(\nabla\cdot\hat{c})(\nabla\times\hat{c}\cdot\hat{z})$ has to be included when the film is both chiral and polar. It is required that the coefficient $|K_{sb}| < 2\sqrt{K_sK_b}$ so that the elastic energy density remains positive for arbitrary splay and bend distortions.

We will restrict ourselves to the hedgehog textures, each containing a central point defect of winding number +1 with core radius ξ. The defect core corresponds to the region in

which $\hat{c}$ is not defined. We assume that its presence affects the elastic energy only through the inner boundary condition at $r=\xi$ and we neglect its energetic contribution when $r<\xi$ [11] where r is the radial distance. The boundary condition is taken to be $\Theta|_{r=\xi}=\varphi+\varphi_d$, where φ is the polar angle in plane-polar coordinates, and φ_d is a constant. This is indeed justifiable for ± 1 defects with the structure discussed in Ref. [12]. We further assume that the defect is stable when it is located at the center of Ω and that the system is cylindrically symmetric, i.e., $\Theta=\varphi+f(\ln r)$, where $f(\ln r)$ is the radial distribution of $\hat{c}$. These assumptions can be shown to be valid for all the textures to be discussed. We shall compute the possible expressions for $f(\ln r)$ that minimize the elastic energy and give the equilibrium textures. In terms of $k\equiv\ln r$, the elastic energy reduces to

$$H[f,f']=\pi\kappa\int_{\ln\xi}^{\ln R_0}dk\{1+f'^2-\mu[(1-f'^2)\cos(2f-2\varsigma_+)-2f'\sin(2f-2\varsigma_+)]\}+2\pi R_0\sigma(-f)|_{\ln R_0}, \quad (2)$$

where $2\kappa\equiv K_s+K_b$, $2\kappa\beta\equiv K_s-K_b$, $2\kappa\tau\equiv K_{sb}$, $\mu\equiv\sqrt{\beta^2+\tau^2}$, $2\varsigma_\pm\equiv\tan^{-1}\tau/\beta\pm\pi$, where R_0 is the radius of the boundary Γ. The equilibrium condition for $f(k)$ is

$$-f''-\mu[f''\cos(2f-2\varsigma_+)-(f'^2+1)\sin(2f-2\varsigma_+)]=0 \quad (3)$$

and the boundary condition at $k=\ln R_0$ is

$$\kappa\{f'+\mu[f'\cos(2f-2\varsigma_+)+\sin(2f-2\varsigma_+)]\}-R_0\sigma'(-f)=0. \quad (4)$$

Depending on the choice of the parameters, f may possess more than one or, at times, numerous solutions. We use linear stability analysis to determine if these solutions are local minima. The elastic energy is expanded to second order in small variations $\chi\equiv f-f_0$ about an equilibrium configuration f_0 as $\delta H=\int dk\chi\mathcal{L}\chi+\psi^T\mathcal{B}\psi$, where

$$\mathcal{L}=-\pi\kappa\left\{[1+\mu\cos(2f_0-2\varsigma_+)]\frac{d^2}{dk^2}-\mu[f_0''\sin(2f_0-2\varsigma_+)+2\cos(2f_0-2\varsigma_+)]\right\}, \quad (5)$$

$$\mathcal{B}_{\chi'\chi'}=0, \quad (6)$$

$$\mathcal{B}_{\chi\chi'}=\mathcal{B}_{\chi'\chi}=\frac{\pi\kappa}{2}[1+\mu\cos(2f_0-2\varsigma_+)]_{\ln R_0}, \quad (7)$$

$$\mathcal{B}_{\chi\chi}=\pi\{-\kappa\mu[f_0'\sin(2f_0-2\varsigma_+)-2\cos(2f_0-2\varsigma_+)]+R_0\sigma''(-f_0)\}_{\ln R_0}, \quad (8)$$

and $\psi^T\equiv(\chi',\chi)|_{\ln R_0}$. The deviation of the elastic energy δH from its equilibrium value can be examined in terms of the eigenvalue λ and associated eigenfunction ϕ_λ satisfying $\mathcal{L}\phi_\lambda=\lambda\phi_\lambda$. The eigenfunctions ϕ_λ are normalized so that $\int dk\phi_\lambda^2=1$ and $\phi_\lambda|_{\ln\xi}=0$ for infinitely strong anchoring at the inner boundary. It is typical in linear stability analysis that there is another boundary condition on ϕ_λ that isolates a set of eigenvalues λ in which the sign of the lowest one is to be tested. For our particular case, there is no other restriction on ϕ_λ that can be imposed and all λ's are allowed. The deviation of energy associated with the fluctuational mode ϕ_λ is no longer λ but

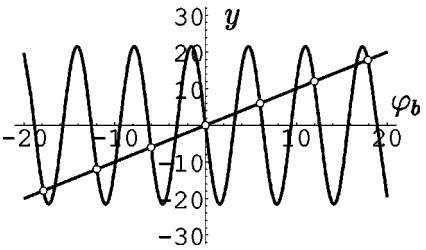

FIG. 1. Plots of $y=\varphi_b$ and $y=R_0a_1(\ln R_0-\ln\xi)\sin\varphi_b/\kappa$ vs φ_b. The intersections, $\varphi_b^{(i)}$, give the equilibrium configurations $f_0^{(i)}(k)$. Those marked with open circles are stable. The parameters used are $\kappa=1$, $R_0=5$, $\xi=0.1$, and $a_1=-1.1$.

$$\delta H_\lambda=\lambda+\psi_\lambda^T\mathcal{B}\psi_\lambda, \quad (9)$$

where $\psi_\lambda^T=(\phi_\lambda',\phi_\lambda)|_{\ln R_0}$. Instability is signified by δH_λ becoming negative. The asymptotic behavior of δH_λ can be shown to be $\delta H_\lambda\sim-|\lambda|+R_0^{(1+2\sqrt{|\lambda|})}$ when $\lambda\to-\infty$, and $\delta H_\lambda>(1-\mathcal{B}_{\chi\chi'}/2\mathcal{B}_{\chi\chi})\lambda$ when $\lambda\to\infty$ for $R_0\sqrt{a_1^2+c_1^2}\gg\kappa$ and $\sigma''(-f_0)|_{k=\ln R_0}\approx\sqrt{a_1^2+c_1^2}$. We see that δH_λ is positive in both limits and can only change sign for small λ.

We have outlined the procedures to obtain the equilibrium textures and to examine their stability against infinitesimal fluctuations. To understand these equilibrium textures, we first look at the simplest case $\beta=\tau=c_1=a_2=\varphi_d=0$ and $a_1<0$. It corresponds to a polar film made of achiral molecules, with isotropic elastic constants and having fixed anchoring at the inner boundary such that $\hat{c}$ points normal into the bulk. The condition $a_1<0$ indicates that $\hat{c}$ favors the outward normal direction at the outer boundary, without being locked. In this case, there are analytic solutions. It is obvious that $f_0(k)=0$ is the lowest-energy configuration: all $\hat{c}$ vectors point along the radial direction. The general solution to $f_0(k)$ is

$$f_0(k)=\frac{\varphi_b}{\ln R_0-\ln\xi}(k-\ln\xi) \quad (10)$$

and φ_b satisfies

$$\varphi_b=\frac{R_0a_1(\ln R_0-\ln\xi)}{\kappa}\sin\varphi_b. \quad (11)$$

The quantity φ_b is the anchoring angle of $\hat{c}$ measured with respect to φ at $k=\ln R_0$. It is easy to see that the system supports numerous equilibrium solutions when the amplitude $|R_0a_1(\ln R_0-\ln\xi)/\kappa|\gg1$. Figure 1 shows the plots of φ_b and $R_0a_1(\ln R_0-\ln\xi)\sin\varphi_b/\kappa$. We denote the solutions of Eq. (11) by $\varphi_b^{(i)}$ with an index i. Not all the solutions are stable. The stable ones are indicated by open circles in Fig. 1. When $\varphi_b^{(i)}\neq0$, we have spirals in which $\hat{c}$ points in the radial di-

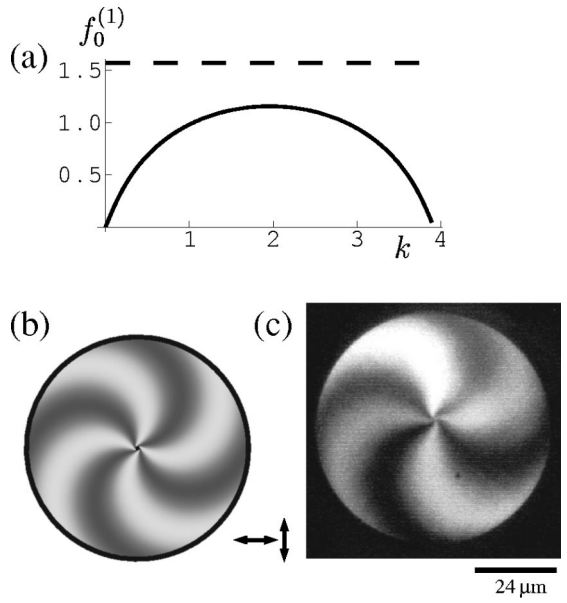

FIG. 2. Illustrations of the lowest-energy configuration for $\kappa=1$, $\mu=0.70$, $\varsigma_+=\pi/2$, $R_0=5$, $\xi=0.1$, $a_2=-10$, and $\varphi_d=0$. (a) is a plot of $f_0^{(1)}(k)$ vs k for $f_0^{(1)'}(0)=1.9788$, the dashed line indicates ς_+, (b) shows the corresponding density plot of $\sin^2\Theta\cos^2\Theta$, and (c) depicts the experimental image of a reversing spiral observed in free standing film of chiral smectic-C liquid crystal. The polarizer and the analyzer are vertical and horizontal.

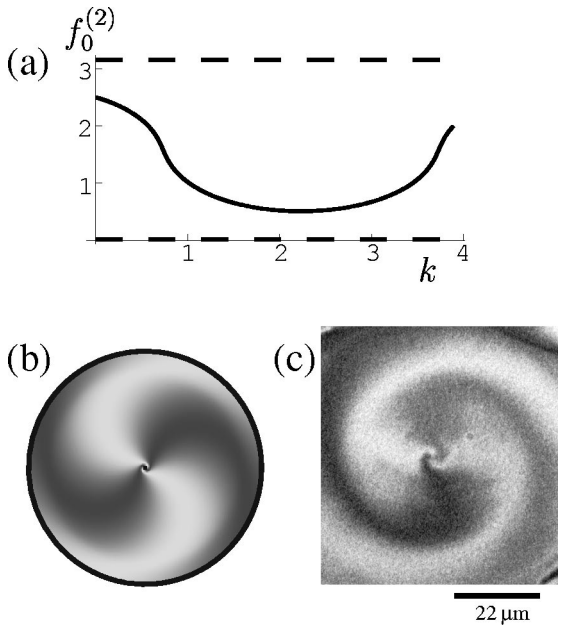

FIG. 3. Illustrations of a texture configuration that resembles the reversing spiral observed experimentally in Ref. [5], when $f_0^{(2)'}(0)=-0.4659$, $\kappa=1$, $\beta=0.90$, $2\varsigma_+=\pi-3.11$, $R_0=5$, $\xi=0.1$, $a_1=10$, $c_1=20$, and $\varphi_d=2.5$. (a) The plot of $f_0^{(2)}(k)$ vs k, the dashed lines indicate ς_+ and $2\pi+\varsigma_-$, (b) the corresponding density plot of $\cos^2\Theta$, and (c) the experimental image of a DRS observed in a chiral smectic-C film on water. Polarizer and analyzer are slightly uncrossed.

rection at the inner boundary and rotates counterclockwise through $\varphi_b^{(i)}$ along a radial path ending at the outer boundary. These metastable textures do not have in-plane reflection symmetry although the system in question is achiral. We find, by inspecting the boundary condition Eq. (11), that there is a solution $\varphi_b^{(j)}=-\varphi_b^{(i)}$ for any solution $\varphi_b^{(i)}$ and these configurations have the same energy. Hence, chiral symmetry is spontaneously broken for the higher-energy metastable configurations. The family of solutions can be classified in terms of a topological index m_i, which is defined to be the nearest integer around $\varphi_b^{(i)}/2\pi$. This classification can also be drawn topologically by examining the possible order-parameter distributions along a line in the radial direction connecting the inner and the outer boundaries [10]. All integers are allowed topologically, but only some are supported energetically in a bounded system.

The situation is different when $a_1>0$, i.e., when the preferred direction of $\hat{c}$ at the outer boundary is in the inward normal direction. The solution $f_0(k)=0$ is now unstable and we cannot have a pure splay texture anymore. The lowest-energy configuration corresponds to the first nonzero $\varphi_b^{(i)}$ satisfying Eq. (11). It is a spiral texture as are all the other metastable configurations allowed. Let us emphasize that they all break the chiral symmetry spontaneously. The spiral textures we have just discussed arise from spontaneously broken chiral symmetry in an isotropic achiral system. The actual system may not be isotropic and the parameter β is not necessarily zero. Further, it is possible to explicitly break the chiral and polar symmetries ($\tau\neq 0$) by adding chiral molecules to the system and by putting the film on water, respectively. When β or τ are nonzero, analytic solutions for Eq. (3) are not obvious and we resort to numerical methods. More complex equilibrium textures with $m_i=0$ are supported in addition to those with higher m_i's. The behavior of the $\hat{c}$- distribution in such cases can be understood intuitively by noting the existence of two preferred bulk directions for $\hat{c}$ when $\Theta-\varphi\in[-\pi,\pi)$, namely, $\Theta_\pm=\varphi+\varsigma_\pm$. Right at the inner boundary of Ω, Θ is set to $\varphi+\varphi_d$. Along a trajectory traversing radially into the bulk, Θ settles smoothly near one of $\Theta_\pm$, depending on which of these gives the lower overall energy of the system (Θ_+ for our case). When it gets to the outer boundary, Θ gradually sets itself at $\varphi+\varphi_b$. The $f_0^{(1)}(k)$ and texture for the lowest-energy configuration taking $\tau\neq 0$, are displayed in Fig. 2. The texture is depicted as the density plot of $\sin^2\Theta\cos^2\Theta$, which simulates the images obtained by a set of crossed polarizers. Figure 2(c) shows an experimental image of a chiral smectic-C liquid-crystal domain in a free standing film. It is very similar to the image shown in Fig. 2(b), computed using the appropriate parameters for a chiral free standing film.

Apparently, these images do not resemble the remarkable and dramatic reversing spiral texture reported in Ref. [5] and shown in Fig. 3(c). Nevertheless, Fig. 2 does represent a reversing spiral, since $f_0^{(1)}(k)$ goes through a maximum at about $k=2.0$. However, the initial rotation of the director near the core is so rapid that it is barely visible. We are able to locate among the various solutions an equilibrium texture that resembles the ''dramatic reversing spiral'' (or DRS texture), illustrated in Fig. 3. The distinguishing feature of the DRS texture is the extended region near the core in which the director rotates slowly. This configuration is constructed by choosing the values of Θ at the inner boundary and at the outer boundary to be around $\Theta_-=\varphi+\varsigma_-+2\pi$. Starting from the inner boundary, Θ first remains near Θ_-, then

swings nearly π to a value close to Θ_+ and finally returns rapidly to $\varphi+\varphi_b$ (which has been set to be around Θ_-) near the outer boundary. The function $f_0^{(2)}(k)$ and its texture are depicted in Fig. 3. There is strong resemblance between the density plot of $\cos^2\Theta$, simulating the images obtained with slightly uncrossed polarizers, and the experimental picture of the DRS.

Remarkably, the DRS is only a metastable texture! It is easy to see that $f_0^{(2)}(k)$ is not the lowest-energy solution. The configuration, in which Θ sets smoothly near Θ_- without going through the rapid changes to Θ_+ and then back to Θ_-, has the lowest-elastic energy. Since $f_0^{(2)}(k)$ is not the global minimum of the elastic energy [Eq. (2)], its stability against fluctuations is in question. We have examined δH_λ, the deviation in energy associated with the reversing spiral solution, in a wide range of λ, and conclude that the DRS is a metastable configuration for the present choice of the parameters. In general, the DRS texture is not even metastable for an arbitrary set of parameters. As noted in Ref. [5], the DRS texture is rare, which is consistent with these findings.

In conclusion, we have analyzed a generic model for textures associated with a $+1$ defect in domains with XY-like ordering. Restricting our analysis to the class of textures with the defect fixed at the center, we find the equilibrium configurations and examine the stability of these configurations against infinitesimal fluctuations. Many metastable configurations are supported at some suitable choice of parameters. These can be classified by a new radial topological number analogous to the winding number classifying the point defect. It is also found that metastable configurations are chiral, including the stable lowest-energy texture when $a_1>0$, even if the system possesses in-plane reflection symmetry. When elastic anisotropy, chirality, and polarity are introduced explicitly, more equilibrium solutions exist. Among the equilibrium textures, we have found two kinds of reversing spirals, simple ones that are absolutely stable textures, and metastable ones of a more dramatic appearance, that resemble closely the reversing spiral reported in Ref. [5].

K.-K. L. would like to express his gratitude to Professor Joseph Rudnick for ideas, suggestions, and support, and to thank Professor Charles Knobler and Professor Robijn Bruinsma for numerous stimulating discussions. This research was supported in part by the NSF through Grant No. DMR-9974388 and by Brandeis University.

[1] J. Ruiz-Garcia, X. Qiu, M.-W. Tsao, G. Marshall, C.M. Knobler, G.A. Overbeck, and D. Möbius, J. Phys. Chem. **97**, 6955 (1993).
[2] X. Qiu, J. Ruiz-Garcia, K.J. Stine, C.M. Knobler, and J.V. Selinger, Phys. Rev. Lett. **67**, 703 (1991).
[3] S. Rivière and J. Meunier, Phys. Rev. Lett. **74**, 2495 (1995); J. Fang, E. Teer, C.M. Knobler, K.-K. Loh, and J. Rudnick, Phys. Rev. E **56**, 1859 (1997).
[4] M.N.G. de Mul and J.A. Mann, Jr., Langmuir **11**, 3292 (1995).
[5] I. Kraus and R.B. Meyer, Phys. Rev. Lett. **82**, 3815 (1999).
[6] T.M. Fischer, R.F. Bruinsma, and C.M. Knobler, Phys. Rev. E **50**, 413 (1994).
[7] D. Pettey and T.C. Lubensky, Phys. Rev. E **59**, 1834 (1999).
[8] D.R.M. Williams, Phys. Rev. E **50**, 1686 (1994).
[9] S.A. Langer and J.P. Sethna, Phys. Rev. A **34**, 5035 (1986).
[10] N.D. Mermin, Rev. Mod. Phys. **51**, 591 (1979).
[11] P.G. de Gennes and J. Prost, *The Physics of Liquid Crystals* (Clarendon, Oxford, 1993), p. 171.
[12] Y. Tabe, N. Shen, E. Mazur, and H. Yokoyama, Phys. Rev. Lett. **82**, 759 (1999).